

Original Paper

Highly Facet-reflection Immune 53GBaud EML for 800G

Artificial Intelligence Optical Transceivers

Jack Jia-Sheng Huang^{1,2}, HsiangSzu Chang², YiChing Hsu², Alex Chiu², ZiHan Fang², Sam Hsiang² & H.S. Chen²

¹ Source Photonics, 8521 Fallbrook Avenue, Suite 200, West Hills, CA 91304, USA

² Source Photonics, No.46, Park Avenue 2nd Rd., Science Park, Hsinchu, Taiwan

Received: October 2, 2023

Accepted: October 19, 2023

Online Published: November 6, 2023

doi:10.22158/asir.v7n4p65

URL: <http://doi.org/10.22158/asir.v7n4p65>

Abstract

We developed a facet-reflection immune 53GBaud electro-absorption modulated laser (EML) for 800G artificial intelligence (AI) optical network. An ultra-low anti-reflection (AR) coating reflectivity of 2×10^{-5} has been demonstrated for straight waveguide. Based on Hakki-Paoli method, we characterized the ultra-low AR using the ripple test technique. Such ultra-low AR is critical in achieving excellent eye pattern and optical transmission for 800G AI supercomputing.

Keywords

Artificial intelligence, AI, 800G optical network, 400G, electro-absorption modulated laser, EML, anti-reflection coating, Hakki-Paoli

1. Introduction

Today, AI plays an important role in manufacturing, electric vehicles, robotics, education, healthcare, and many other areas. Recently, the AI applications have been accelerated by companies such as Nvidia and OpenAI. The launch of ChatGPT in November 2022 has planted seeds for business growth of AI (Lock, 2022). In mid-May 2023, Nvidia released the DGX H200 supercomputer for AI, leading to reshaping of industry demand with 800G optical transceiver orders pouring in (Fibermall, 2023). Since then, other tech giants like Google, Meta, Microsoft and Amazon are also considering integrating AI into their operations, thereby driving the implementation of the AI industry chain both upstream and downstream (Kozlov, 2023).

800G AI has achieved remarkable progress in information processing, data analysis, and decision-making (Jason, 2023). With a processing capability of 800 gigabits per second (Gbps), the 800G AI is poised to expand the frontiers of computational intelligence. As data volumes explode and

demand for real-time insights intensifies, 800G AI has emerged as a central source in enabling seamless, high-speed data computation and machine learning applications across industries such as finance, healthcare, and manufacturing.

53GBaud EML provides the core computing power of 800G AI optical transceiver (Wang, 2023; Huang et al., 2017; Takemi, 2022). By using 4-level pulse-amplitude modulation (PAM4), the data rate can be doubled from the traditional 2-state non-return-to-zero (NRZ) modulation to the modern 4-state PAM4. In the PAM4 data transmission algorithm, 53GBaud EML is capable of supporting 100G per single lambda. In addition, 400G and 800G optical transmissions can be realized when 4 and 8 PAM4 channels of 53GBaud EMLs are deployed in optical transceivers, respectively (Huang et al., 2016; Okuda et al., 2021; Honda et al., 2023). The 53GBaud EML's ability to encode, modulate, and transmit data across vast distances with minimal signal degradation positions it as a game-changer in the world of telecommunications and datacenter networking.

EML is the key source laser in the 800G AI transceiver due to its performance advantages of high speed, high extinction ratio and high power over directly modulated laser (DML), silicon photonics (SiPh) and vertical cavity surface emitting laser (VCSEL) (Huang et al., 2016; Okuda et al., 2021; Honda et al., 2023; Huang & Jan, 2016). To meet high-volume manufacturing, several key technical challenges including (1) low reflection, (2) high bandwidth, (3) self-hermeticity, and (4) robust reliability need to be addressed. In this paper, we focus on the facet reflection improvement that is crucial to the radio frequency (RF) noise and fiber dispersion (Miyazaki et al., 2006; Miyazaki et al., 2002; Raring et al., 2007). One method to mitigate the reflection issue is by employing a very low reflectivity optical coating (<0.01%) on the front facet. In this paper, we report a facet-reflection immune 53GBaud EML device based on ultra-low AR coating in the order of 10^{-5} . We characterize the ultra-low reflectivity coating by using the ripple test technique deriving from Hakki-Paoli method (Hakki & Paoli, 1973; Kaminow, Eisenstein & Stulz, 1983). We show that the ultra-low laser reflection is very influential to the 800G AI optical transmission.

2. Experimental

Figure 1 shows the illustrative schematics of artificial intelligence applications and optical networks. AI operations require massive amounts of computing capabilities. To fulfill such supercomputing, the AI servers need graphics processing units (GPU) and optical transceivers. For example, each Nvidia's DGX H100 server integrates eight H100 GPUs and eight 800G OSFP optical transceivers (Holly, 2023).

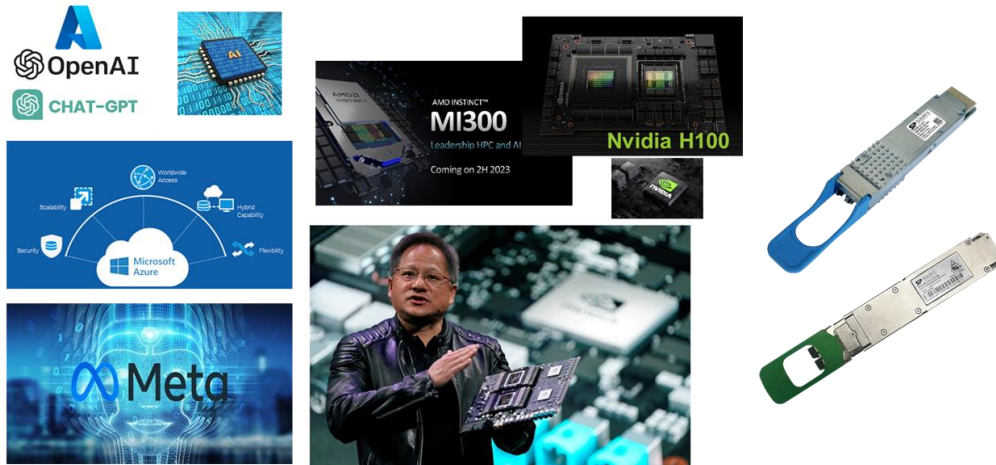


Figure 1. Illustration of AI Applications where GPU and 800G Optical Transceivers are Important Building Blocks for the AI Servers and Supercomputers

Figure 2 shows the cross-sectional schematic of a 53GBaud monolithic, integrated EML structure for 400G and 800G AI optical transceivers. The front section of the EML device is the electro-absorption modulator (EAM) for RF modulation, and the rear section is the distributed feedback laser diode (DFB-LD) for light source. The LD and EAM are monolithically joined by using butt-joint (BJ) technology (Huang et al., 2016). The two sections are separated by an isolation region. For both LD and EAM, the quaternary InGaAsP multi-quantum well (MQW) and separate confinement (SCH) structures were grown by metal organic chemical vapor deposition (MOCVD). The SiO₂ dielectric layer was deposited for passivation. In the EAM section, a low-k polyimide was also deposited to reduce the capacitance. The dielectric layers were etched in the contact opening process to make ohmic contact with Ti/Pt/Au p-metal (Huang et al., 2003).

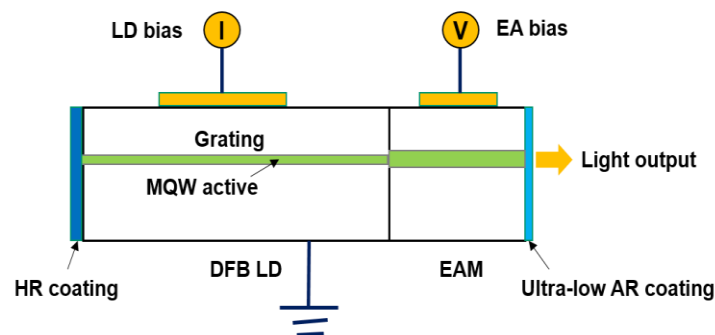


Figure 2. Schematic of Monolithic, Integrated 53GBaud EML Device. The Front is the EAM for RF Modulation; the Back is the DFB for Light Source

To minimize facet reflection, the EML chip is coated with an ultra-low AR coating where reflectivity is in the order of 10^{-5} to 10^{-4} . The AR coating was deposited on the laser facet by ion beam sputtering (IBS) to achieve ultra-low reflectivity and self-hermetic film quality. Due to the test resolution limitation of the

conventional filmetrics (Filmetrics, 2013), we developed a new ripple test technique based on Hakki-Paoli method to estimate the AR reflectivity.

The EML chip was mounted to a carrier before direct current (DC) and RF test characterization. The LD section was biased with DC current from 0 to 150mA. Upon constant LD bias, the EAM section was tested with a reverse voltage bias ranging from 0 to -3V. Based on the plot of fiber power versus EAM voltage, extinction ratio (ER) can be extracted based on the ON and OFF states. The voltage swing between the ON and OFF states was 1V.

3. Results and Discussion

A. EML device characteristics

Figure 3 shows the typical light versus current (LI) curve of a 53GBaud EML device where the modulator was not biased. When the modulator was set at 0V, 53°C, there was essentially no light absorption from the modulator section. So, the output power of the laser section was fully collected by the LI measured from the front facet of the EAM. The threshold current (I_{th}) taken from the LI was about 14mA.

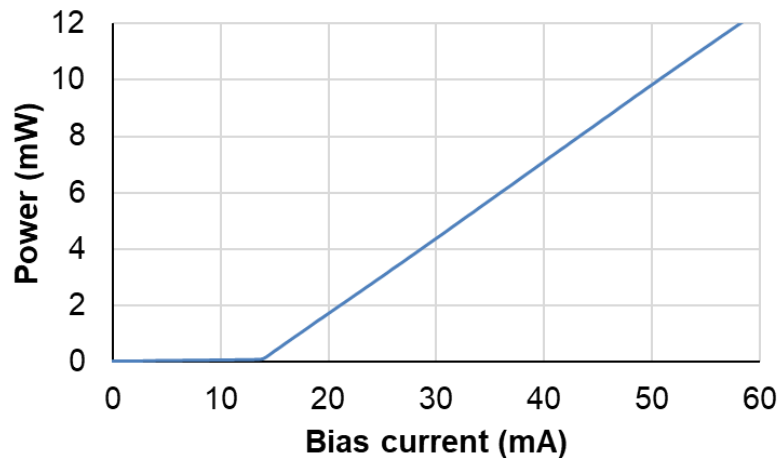


Figure 3. Typical LI Curve of the 53GBaud EML Device where the EAM Section is at OFF State with no Bias at 53°C

Figure 4 shows the output power curve of a 53GBaud EML device as a function of EAM bias at 53°C. As the EAM section was subjected to reverse bias, light absorption by the EA modulator started to occur. The light absorption from the modulator increased with increasing reverse voltage. As the magnitude of reverse voltage became larger, the power decreased due to larger light absorption. The ER is proportional to the slope shown in the box during the voltage swing. For example, the voltage swing at 1.0V where the V_{ON} and V_{OFF} are 0.5V and 1.5V, respectively. Using the same method, we can extract ER value at different EAM voltages to compile a full ER curve.

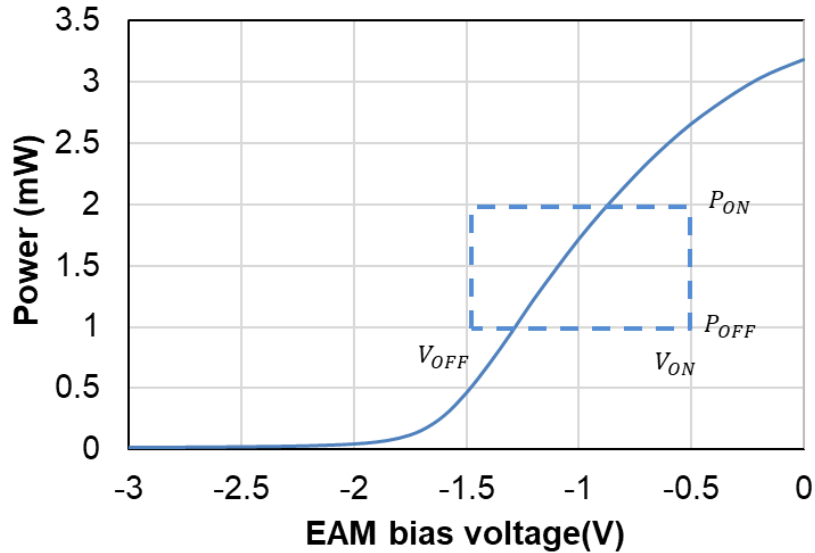


Figure 4. Typical Fiber-coupled Power Curve of the 53GBaud EML Device where the EAM Section is Subjected to the Reverse Voltage up to -3V at 53°C. The ER can be Extracted from the EA Absorption Curve where the Voltage Swing between ON and OFF States are Indicated

With the establishment of the EA absorption curve, we can determine the ER based on 1.0V of voltage swing. Figure 5 shows the typical ER curve of a 53Gaud EML device as a function of EAM bias. At low reverse voltage, the slope of the power curve was low, and the resultant ER was lower. The ER value was relatively high in the range of -0.8 to -1.5V and reached the maximum near -1.2V. At high voltage, the slope and ER became low again. The ER curve based on DC chip testing could provide a good prescreening for the final transceiver test. We estimated that such high ER at the chip level would be sufficient for 400G and 800G optical transmission.

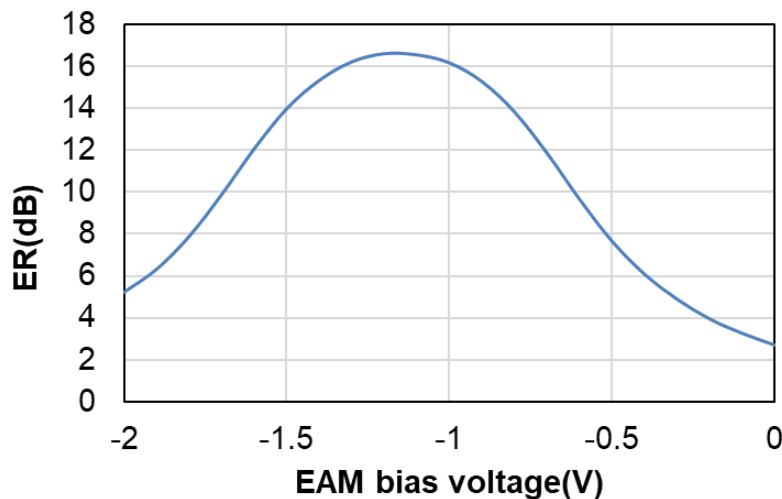


Figure 5. Typical ER Curve of the 53GBaud EML Device as a Function of EAM Bias, Measured by DC Chip Testing at 53°C

It was also noted that there was a tradeoff between the ER and power. At the reverse voltage of 0V, the power was the highest while the ER was not at maximum. As the reverse voltage ramped up at around -1.2V, the ER reached the maximum while the power decreased. The overall optimal operating point of EML was typically determined by the balance between the ER and power.

Figure 6 shows the typical optical spectra of 53GBaud EMLs of coarse wavelength division multiplexing (CWDM) at 53°C. Each EML channel exhibits good single-mode DFB performance with the side-mode-suppression-ratio (SMSR) over 50dB. The side mode immediately next to the main DFB peak was from the stopband that was dependent on the grating strength. The small ripples were from the Fabry-Perot where the spacing depended on the cavity length. The peak-to-peak amplitude of the FP ripple was related to the coating reflectivity that will be discussed in the next section. To meet IEEE802.3 specifications, 800G 2xFR4 uses center wavelengths of 1271, 1291, 1311 and 1331nm for CWDM channels (L0, L1, L2 and L3, respectively) (Welch, 2023; Wang, 2023). 800G DR8 uses eight EMLs with a center wavelength of 1311nm.

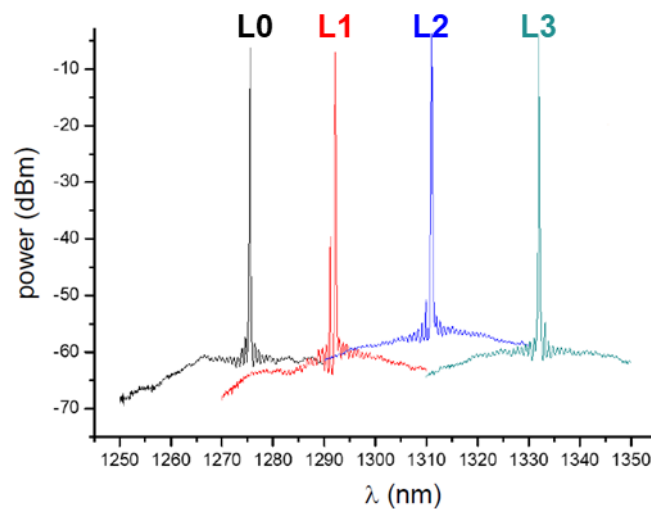


Figure 6. Typical Optical Spectra of 53GBaud CWDM EML Devices Showing Good Single-mode DFB Performance at Each Wavelength

Figure 7 shows the frequency response plot of 53GBaud EML. The 3dB bandwidth reached about 40 GHz, well above the specification of 35 GHz. The ultra-low AR also helped achieve good S21 flatness.

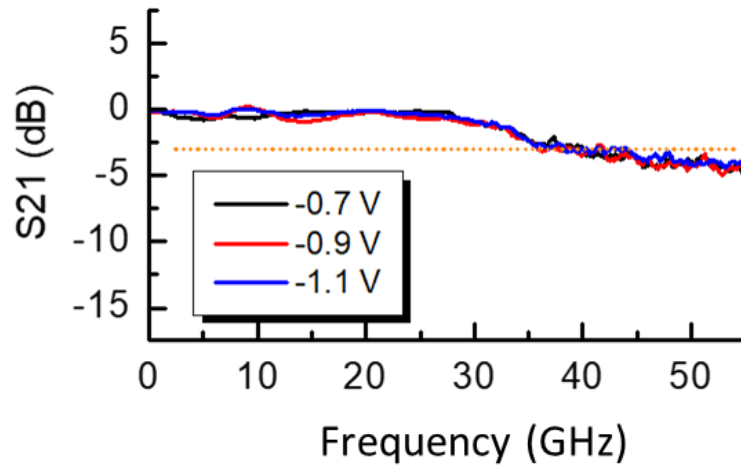


Figure 7. Frequency Response Curve of the 53GBaud EML Device Showing High 3dB Bandwidth (~40 GHz) and Good S21 Flatness

Figure 8 shows the PAM4 eye pattern of 400G optical transceiver. The 53GBaud EML chips showed excellent eye opening in the 400G transceiver where the transmitter dispersion eye closure quaternary (TDECQ) reached as low as 1.1 dB. TDECQ is an important index to evaluate the optical emission communication quality of PAM4 (King, 2016; Fibermall, 2023). It measures the extra noise ratio when the transmitter and the ideal transmitter get the same bit error rate. A smaller the TDECQ value indicates a better and more robust optical signal quality. The typical target of TDECQ is ≤ 3.4 dB. Our 53G EMLs also demonstrate excellent versatility and extendibility with modern 800G data transmission systems. Table I shows the ER and TDECQ of the 53GBaud EMLs in 400G and 800G optical transceivers. The TDECQ values in both applications are favorably less than 2 dB while maintaining the ER above 5 dB. We show that our 53GBaud EML devices well exceed all the performance specifications of 400G and 800G AI applications.

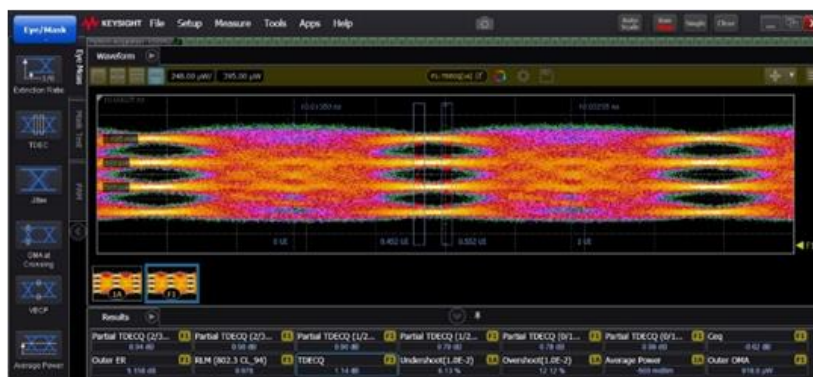


Figure 8. PAM-4 Eye Pattern of the 53GBaud EML Device in a 400G Optical Transceiver. The Eye Diagram Showed Excellent Opening with TDECQ as Low as 1.1 dB

Table 1. ER and TDECQ of the 53GBaud EMLs in 400G and 800G Optical Transceivers.

Optical modules	ER (target \geq 3.5 dB)	TDECQ (target \leq 3.4dB)
400G DR4 & FR4	5.3 dB	1.4 dB
800G DR8 & 2xFR4	5.0 dB	1.9 dB

B. Ultra-low AR characterization

The conventional method to measure coating reflectivity is by means of reflectance spectrum where the peak and valley are based on in-phase and out-of-phase signals (Hind & Perier, 2011). The working principle of the reflectance measurement is based on the light interaction between the reflections from the top and bottom interfaces of the coating film. Although the conventional technique is simple to implement, it imposes test resolution limitation that occurs around 10^{-3} .

In order to characterize the coating reflectivity at ultra-low regime ($<10^{-4}$), we utilized the amplified spontaneous emission (ASE) ripple test based on Hakki-Paoli method (Hakki & Paoli, 1973; Kaminow, Eisenstein & Stulz, 1983). Consider a semiconductor laser with a cavity length of L bounded by mirrors of front and back coating reflectivities R_1 and R_2 , the change in the propagating light power after a round trip can be expressed in Equation (1) where $P(0)$ is the initial light power, $P(2L)$ is the light power after round trip of $2L$, g is the gain coefficient and α is the loss coefficient in the unit of cm^{-1} (Fukuda, 1999).

$$\frac{P(2L)}{P(0)} = R_1 R_2 \exp[2L(g - \alpha)] \quad (1)$$

By employing the Hakki-Paoli method, the ASE ripple can be related to the coating reflectivity as follows.

$$\ln(a) = gL\left(\frac{I}{I_{th}}\right) - \left(gL - \ln \frac{\sqrt{R_1 R_2}}{R_1}\right) \quad (2)$$

where a is the ASE ripple, I is the bias current, and I_{th} is the laser threshold current. The ASE ripple (a) is a function of peak-to-peak amplitude taken from the ASE spectrum, as shown in Equation (3) (Kaminow, Eisenstein, & Stulz, 1983; Lorch, 2003; Meritt et al., 1995).

$$\frac{2a}{1+a^2} = \frac{\sqrt{r}-1}{\sqrt{r}+1} \quad (3)$$

Figure 9 shows the example of ASE ripple from the front coating mirror of an FP test structure measured at a bias current below the threshold current ($0.8 \times I_{th}$) at 25°C . The median value of the ripple was 1.28dB, corresponding to the AR coating reflectivity (R_1) of 2×10^{-5} . The reflectivity of the highly

reflective (HR) in the rear coating mirror (R_2) was fixed at 95%. The gain and loss coefficients were assumed to be 80 and 20 cm^{-1} , respectively.

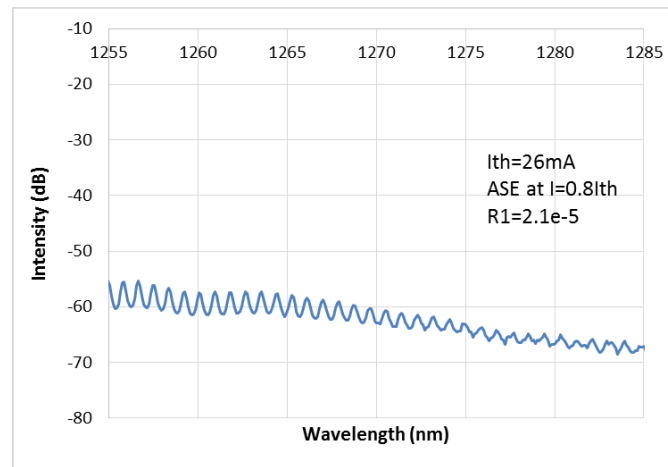


Figure 9. ASE Spectra of Ultra-low AR Coating Measured at Bias Current of $0.8I_{th}$. The Ripple is 1.3dB, Corresponding to the Reflectivity R_1 of 2×10^{-5}

4. Conclusion

We have developed a facet-reflection immune 53GBaud EML for 400G and 800G AI optical networks. An ultra-low AR coating reflectivity of 2×10^{-5} has been successfully fabricated to reduce the RF noise and chirp. Based on Hakki-Paoli method, we characterized the ultra-low AR by using the ripple test technique. The high-speed, low reflection 53GBaud EML can meet the stringent performance requirements of 800G AI supercomputing. The 53GBaud EML lasers of CWDM (1271, 1291, 1311 and 1331nm) can support 400G DR4, 400G FR4, 800G DR8 and 800G 2xFR4.

Acknowledgments

The authors would like to thank Source Photonics Taiwan Fab Production Engineering team (Hsinchu, Taiwan) for wafer processing and testing as well as Source Photonics Module team (Chengdu, China) for optical transceiver data. Ashley Huang (UCD, Davis, CA) and Shannon Huang (UCLA, Los Angeles, CA) are acknowledged for editing and proofreading.

References

- Fibermall (2023). NVIDIA and 800G Optical Transceiver Module. *Fibermall*.
<https://www.fibermall.com/blog/nvidia-and-800g-optical-transceiver-module.htm>
- Fibermall. (2023). What is TDECQ. <https://www.fibermall.com/blog/what-is-tdecq.htm>
- Filmetrics. (2013). Operations Manual for the FILMETRICS F20 Thin-Film Analyzer (Filmetrics Corporation, San Diego, CA), Revision 7.4.0.0.
- Fukuda, M. (1999). Optical semiconductor devices (New York, NY, Wiley), Chapter 3.

- Hakki, B. W., & Paoli, T. L. (1973). CW degradation at 300K of GaAs double-heterostructure junction lasers-II: electronic gain. *J. Appl. Phys.*, *44*, 4113-4119. <https://doi.org/10.1063/1.1662905>
- Hind, A. R., & Perier, C. (2011). Low reflectance measurements using the 'VW' technique. Agilent Technologies Application Note SI-A-1220
- Holly. (2023). AI computing power boosts 800G optical transceiver demand growth. *NADDOD*. <https://www.naddod.com/blog/ai-computing-power-boosts-800g-optical-transceiver-demand-growth>
- Honda, M., Tamura, A., Takada, K., Sakurai, K., Kanamori, H., & Yamaji, K. (2023). 53Gbaud electro-absorption modulator integrated lasers for intra-data center networks. *Sumitomo Electric Technical Review*, *96*, 20-24. <https://www.sourcephotonics.com/news/fs-tunes-up-source-photonics-800g-transceivers-for-scaling-data-center-connectivity/>
- Huang, J. S., & Jan, Y. H. (2016). Interconnected analogy and resemblance: from classical music to modern semiconductor technology. *Int'l J. Electrical Electron. Eng.*, *5*(2), 1-8.
- Huang, J. S., & Vartuli, C. B. (2003). Scanning electron microscopy study of Au/Zn/Au/Cr/Au and Au/Ti/Pt/Au/Cr/Au contacts to p-type InGaAs/InP. *J. Appl. Phys.*, *93*, 5196-5200. <https://doi.org/10.1063/1.1565187>
- Huang, J.S., Jan, Y.H., Chang, H.S., Chang, J., Chang, R., Liu, G., Ren, D., & Chou, E. (2017). ESD polarity effect study of monolithic, integrated DFB-EAM EML for 100/400G optical networks. *CLEO-PR* (Singapore, July31-Aug.4), Paper#S1018. <https://doi.org/10.1109/CLEOPR.2017.8118609>
- Huang, J.S., Jan, Y.H., Chang, J., Hsu, Y.C., Ren, D., & Chou, E. (2016). Swift reliability test methodology of 100G high-speed, energy-efficient electro-absorption modulated lasers (EML) for green datacenter networks. *Studies Eng. Tech.*, *3*(1), 74-80. <https://doi.org/10.11114/set.v3i1.1727>
- Jason (2023). The New Era of 800G Optical Transceiver. *Naddod*. <https://www.naddod.com/blog/800g-optical-transceiver-new-era>
- Kaminow, I. P., Eisenstein, G., & Stulz, L. W. (1983). Measurement of the modal reflectivity of an antireflection coating on a superluminescent diode. *IEEE J. Quantum Electron.*, *QE-19*(4), 493-495. <https://doi.org/10.1109/JQE.1983.1071887>
- King, J. (2016). TDEC for PAM4 ('TDECQ'). *IEEE802.3*, 29-37.
- Kozlov, V. (2023). AI creates a new wave in demand for optical transceivers. *Lightcounting*.
- Lock, S. (2022). What is AI chatbot phenomenon ChatGPT and could it replace humans? *The Guardian*.
- Lorch, S. (2003). Theory and Measuring of Antireflection Coatings. Annual Report, *Optoelectronics Department, University of Ulm*, 1-6.

- Merritt, S.A., Dauga, C., Fox, S., Wu, I.-F., & Dagenais, M. (1995). Measurement of the facet modal reflectivity spectrum in high quality semiconductor traveling wave amplifiers. *J. Lightwave Tech.*, 13(3), 430-433. <https://doi.org/10.1109/50.372438>
- Miyazaki, Y., Tada, H., Aoyagi, T., Nishimura, T., & Mitsui, Y. (2002). Extremely small-chirp electroabsorption-modulator integrated distributed feedback laser diode with a shallow quantum-well absorption layer. *J. Quantum Electron.*, 38(8), 1075-1080. <https://doi.org/10.1109/JQE.2002.801030>
- Miyazaki, Y., Yamatoya, T., Matsumoto, K., Kuramoto, K., Shibata, K., Aoyagi, T., & Ishikawa, T. (2006). High-power ultralow-chirp 10-Gb/s electroabsorption modulator integrated laser with ultrashort photocarrier lifetime. *J. Quantum Electron.*, 42(4), 357-362. <https://doi.org/10.1109/JQE.2006.870228>
- Okuda, S., Yamatoya, T., Yamaguchi, T., Azuma, Y. & Tanaka, Y. (2021). High-power low-modulating-voltage 1.5 m-band CWDM uncooled EMLs for 800 Gb/s (53.125 Gbaud-PAM4) transceivers, *OFC 2021 Tu1D.2*. <https://doi.org/10.1364/OFC.2021.Tu1D.2>
- Raring, J.W., Johansson, L.A., Skogen, E.J., Sysak, M.N., Poulsen, H.N., DenBaars, S.P., & Coldren, L. A. (2007). 40-Gbs/s widely tunable low-drive-voltage electroabsorption-modulated transmitters. *J. Lightwave Tech.*, 25(1), 239-248. <https://doi.org/10.1109/JLT.2006.886722>
- Takemi, M. (2022). High frequency and optical devices. *Mitsubishi Electric Advances*, 177.
- Wang, J. (2023). FS Tunes up Source Photonics' 800G Transceivers for Scaling Data Center Connectivity.
- Wang, J. (2023). Source Photonics surpasses 2.5 million mark in high speed 28G/53G EML chip shipments and adds 100G EML chips to its market leading EML portfolio. <https://www.sourcephotonics.com/news/source-photonics-surpasses-2-5-million-mark-in-high-speed-28g-53g-eml-chip-shipments-and-adds-100g-eml-chips-to-its-market-leading-eml-portfolio/>
- Welch, B. (2023). Baseline Proposals for 800GBASE-DR4, 800GBASE-DR4-2, and 800GBASE-FR4. *IEEE P802.3df 200 Gb/s, 400 Gb/s, 800 Gb/s, and 1.6 Tb/s Ethernet Task Force*.